

Coherent π^0 photoproduction at intermediate energy

J. H. Koch

*National Institute for Nuclear Physics and High Energy Physics,
Amsterdam, The Netherlands*

E. J. Moniz

*Center for Theoretical Physics, Laboratory for Nuclear Science and Department of Physics,
Massachusetts Institute of Technology, Cambridge, Massachusetts 02139*

(Received 20 September 1982)

Coherent π^0 photoproduction from nuclei is calculated in the Δ -hole framework. Important background production terms are included, and a comparison with data is presented. Sensitivity to various aspects of the dynamics, such as recoil and the Δ spreading potential, are examined.

NUCLEAR REACTIONS ${}^4\text{He}, {}^{12}\text{C}(\gamma, \pi^0)$ calculated in Δ -hole formalism and compared with data for $E_\gamma = 200$ to 400 MeV.

I. INTRODUCTION

Coherent π^0 photoproduction from nuclei is a very attractive reaction for testing and extending our knowledge about pion production and propagation in the nuclear medium. On one hand, this reaction offers information beyond that obtained from analyses of pion elastic scattering data. On the other hand, the reaction amplitude is, in principle, unambiguously calculable within the framework of a microscopic model of the pion-nucleus optical potential (only the "elastic channel" pion wave function is needed). Since π^0 production proceeds dominantly at medium energy via Δ excitation, studies of the nuclear coherent production mechanism can test and perhaps refine the picture of Δ -nucleus interactions derived from analyses of pion elastic scattering. Nevertheless, rather little effort, experimental or theoretical, has been expended on studies of coherent π^0 photoproduction. The experiments are clearly difficult, so that no systematic data set, spanning a variety of energies and targets, exists yet. This situation will likely change in the near future, with several new measurements in progress or planned at various accelerators. In anticipation of this, we present here theoretical results for the light targets ${}^4\text{He}$ and ${}^{12}\text{C}$ and compare them with the existing data. The calculations are performed within the microscopic Δ -hole approach applied with considerable success to pion elastic scattering from the same targets. Our goal is to clarify the extent to which a fairly refined dynamical model agrees or disagrees with existing data and thereby to provide some guidance

for future experimental programs. We also provide some measure of the present theoretical uncertainty in evaluating the reaction amplitude.

There have been a few other calculations of coherent π^0 photoproduction, focusing upon the role of the Δ . We previously presented results for ${}^{16}\text{O}(\gamma, \pi^0){}^{16}\text{O}$ in the isobar-hole formalism,¹ using a very simple production operator (Δ only) and focusing mainly on the formal aspects of the theory, such as reliability of the distorted wave impulse approximation. In the current work, we incorporate the very important background production terms, use a refined Δ -nucleus interaction model (e.g., including a Δ -nucleus spin-orbit potential), and compare directly with data. Oset and Weise² and Klingenberg and Huber³ have also performed calculations with a microscopic Δ -hole model, although there are a number of differences, both in the model and in the evaluation, compared to our calculations. Saharia and Woloshyn⁴ calculate coherent π^0 photoproduction using a phenomenological or parametrized Δ -hole amplitude.

The paper is organized as follows. Our model for the elementary production amplitude $\gamma N \rightarrow \pi^0 N$ is discussed in Sec. II. The Δ -hole formalism for nuclear coherent photoproduction is presented in Sec. III. Comparisons with data are presented and sensitivities to various dynamical mechanisms are discussed in Sec. IV. In the last section, the calculations of Refs. 2–4 are discussed and conclusions from this and from the comparisons with data are drawn. Suggestions for future experimental and theoretical work are put forward.

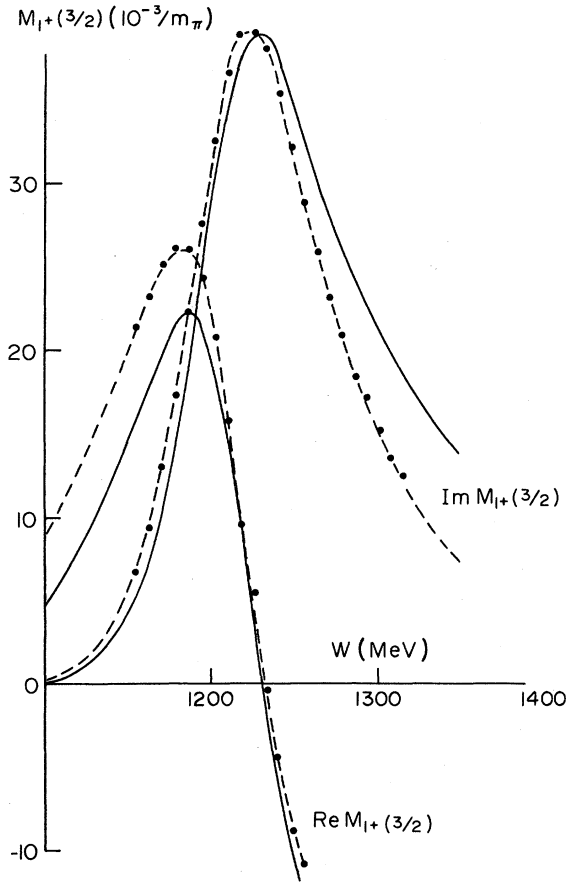


FIG. 1. Energy dependence of the $M_{1+}(\frac{3}{2})$ resonant multipole. Data from Berends and Donnachie (Ref. 6). Solid line is the fit with the Δ only [Eq. (5)]. Dashed line includes background [Eqs. (10) and (11)].

II. THE ELEMENTARY PHOTOPRODUCTION AMPLITUDE

The excitation of the Δ resonance in the $M_{1+}(\frac{3}{2})$ channel provides the dominant contribution to intermediate energy π^0 photoproduction from the nucleon. In the center of mass (c.m.) frame, the amplitude has the form

$$M_{\Delta} = F_{\pi N \Delta}^{\dagger} \frac{1}{D(E)} F_{\gamma N \Delta}, \quad (1)$$

where the magnetic dipole photon coupling to the Δ is described by

$$F_{\gamma N \Delta} = \frac{g_{\gamma N \Delta}}{M_{\Delta}} \hat{\epsilon}_{\vec{k}\lambda} \times \vec{k} \cdot \vec{S}^{\dagger} T_3^{\dagger} \quad (2)$$

with \vec{S}^{\dagger} and T_3^{\dagger} the $N \rightarrow \Delta$ transition spin and isospin operators, respectively. The pion coupling has the longitudinal p -wave form

$$F_{\pi N \Delta}^{\dagger} = \frac{g_{\pi N \Delta}}{M_{\pi}} \vec{q} \cdot \vec{S} T_{\alpha} v(q^2), \quad (3)$$

$$v(q^2) = [1 + q^2/\alpha^2]^{-1}.$$

The resonant denominator is written in terms of the πN 3-3 scattering phase shift

$$\begin{aligned} D(E) &= E - E_R(E) + i\Gamma(E)/2 \\ &= \frac{\Gamma(E)}{2} [i - \cot\delta_{33}(E)]. \end{aligned} \quad (4)$$

With this parametrization, the amplitude automatically has the scattering phase, consistent with the requirements of the Watson final state theorem,⁵

$$M_{\Delta} = e^{i\delta_{33}(E)} \left\{ -F_{\pi N \Delta}^{\dagger} \frac{\sin\delta_{33}}{\Gamma/2} F_{\gamma N \Delta} \right\}. \quad (5)$$

We take the parameters

$$g_{\gamma N \Delta} = 1.02 \quad (6a)$$

and, from pion scattering,

$$\begin{aligned} g_{\pi N \Delta}^2/4\pi &= 0.90, \\ \alpha &= 300 \text{ MeV}/c. \end{aligned} \quad (6b)$$

The resulting Δ contribution to the resonant $M_{1+}(\frac{3}{2})$ multipole is shown in Fig. 1. While the overall qualitative behavior of the multipole is given, a substantial discrepancy remains, especially below the resonance.

The discrepancy between M_{Δ} and the experimental $M_{1+}(\frac{3}{2})$ multipole⁶ arises from the neglect of background terms. We will not need to know the detailed structure of the background production term. Our approach in the nuclear calculation will be to treat the dominant Δ propagation with great care, including the medium modifications found important in pion scattering. However, background production will be treated only in impulse approximation, so that a convenient parametrization of this contribution is sufficient. We follow the same procedure as that used by Olsson⁷ and by Blomqvist and Laget.⁸ The full $M_{1+}(\frac{3}{2})$ multipole amplitude is now written as

$$\begin{aligned} M_{1+}(\frac{3}{2}) &\equiv M_B^{1+}(\frac{3}{2}) + \tilde{M}_{\Delta}^{1+}(\frac{3}{2}) \\ &= F_{\pi N \Delta}^{\dagger} \left\{ \mathcal{A}_B + \frac{e^{i\phi(E)}}{D(E)} \right\} F_{\gamma N \Delta}. \end{aligned} \quad (7)$$

The term \mathcal{A}_B represents background production in the resonant channel. Since the channel quantum numbers determine the spin-isospin structure, we write this term proportional to $F_{\pi N \Delta}^{\dagger} F_{\gamma N \Delta}$. To satisfy unitarity, we must modify the Δ term. Clearly

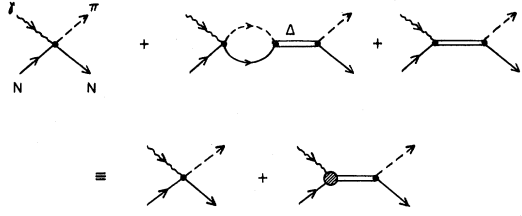


FIG. 2. Schematic representation of pion photoproduction in the resonant multipole. The dot represents non-resonant production (Born terms) in the $M_{1+}(\frac{3}{2})$ channel. The second term in the first line corresponds to resonant rescattering of the photoproduced pion. The cross-hatched circle in the second line corresponds to an effective $\gamma N \Delta$ vertex [see Eq. (7)].

we could not satisfy Watson's theorem by merely adding the background terms and M_Δ . The physical origin of the modification $e^{i\phi(E)}$ is the interference term generated by producing the πN system through the background mechanism and then having the πN system scatter via the Δ . This is indicated in Fig. 2. We choose to incorporate this effect by multiplying M_Δ in Eq. (7) by the complex phase factor $\exp(i\phi(E))$:

$$\tilde{M}_\Delta^{1+} = e^{i\phi(E)} M_\Delta^{1+}. \quad (8)$$

The constraint of Watson's theorem then fixes the background amplitude to be

$$\mathcal{A}_B = -\frac{\sin\phi(E)}{\Gamma(E)/2}, \quad (9)$$

so that we can write

$$M_{1+}(\frac{3}{2}) = -e^{i\delta_{33}(E)} F_{\pi N \Delta}^\dagger \frac{\sin(\delta_{33} + \phi)}{\Gamma(E)/2} F_{\gamma N \Delta}. \quad (10)$$

Finally, the phase ϕ is fit to the experimental multipole with a form consistent with the correct low energy behavior

$$\phi(E) = \frac{q^3}{a_1 + a_2 q^2} \quad (11)$$

(in deg), where q is the pion c.m. momentum, $a_1 = 0.0222 \text{ fm}^{-3}$ and $a_2 = 0.0778 \text{ fm}^{-1}$. This fit is shown by the dashed lines in Fig. 1. Note that the phase ϕ advances the position of the peak of the imaginary part in Fig. 1 by about 10° , as required by the data. It also yields a large increase in the cross section below the resonance.

To complete our description of the single nucleon amplitude $M_{\gamma\pi^0}$, we also have to include the remaining background amplitudes M_B :

$$M_{\gamma\pi^0} = M_B + M_{1+}(\frac{3}{2}). \quad (12)$$

These multipoles are small and have little effect on the total $\gamma N \rightarrow \pi^0 N$ cross section. However, the angular distributions are modified appreciably at low energy because of interference with the $M_{1+}(\frac{3}{2})$ multipole. In Fig. 3, we show the $\gamma p \rightarrow \pi^0 p$ cross section at several energies⁹⁻¹⁸ together with the cross section generated by the Berends and Donnachie⁶ multipoles; we use these multipoles in our calculation of nuclear photoproduction. There are few data for π^0 photoproduction in the forward direction at lower energies. As is clear from Fig. 3, the multipole prediction does not agree well with the forward distribution at low energy. Similar problems also show up in the effective Lagrangian approach of Ref. 8. The origins of this discrepancy are not known, although it is clear that the data have considerable uncertainty. This ambiguity in the elementary cross section will propagate directly to our calculations of coherent π^0 photoproduction and will be discussed again in Sec. IV.

III. THE NUCLEAR PHOTOPRODUCTION AMPLITUDE

First, we write the coherent π^0 photoproduction amplitude corresponding to Δ excitation only. This has a formal structure very similar to Eq. (1):

$$\begin{aligned} \langle \vec{q}; 0 | T_\Delta | \vec{k}, \lambda; 0 \rangle &= \langle \vec{q}; 0 | F_{\pi N \Delta}^\dagger \frac{1}{D(E - H_\Delta) - \delta W - W_\pi - V_{sp}} F_{\gamma N \Delta} | \vec{k}, \lambda; 0 \rangle \\ &\equiv \langle \vec{q}; 0 | F_{\pi N \Delta}^\dagger \frac{1}{D(E) - H_{\Delta h}} F_{\gamma N \Delta} | \vec{k}, \lambda; 0 \rangle, \end{aligned} \quad (13)$$

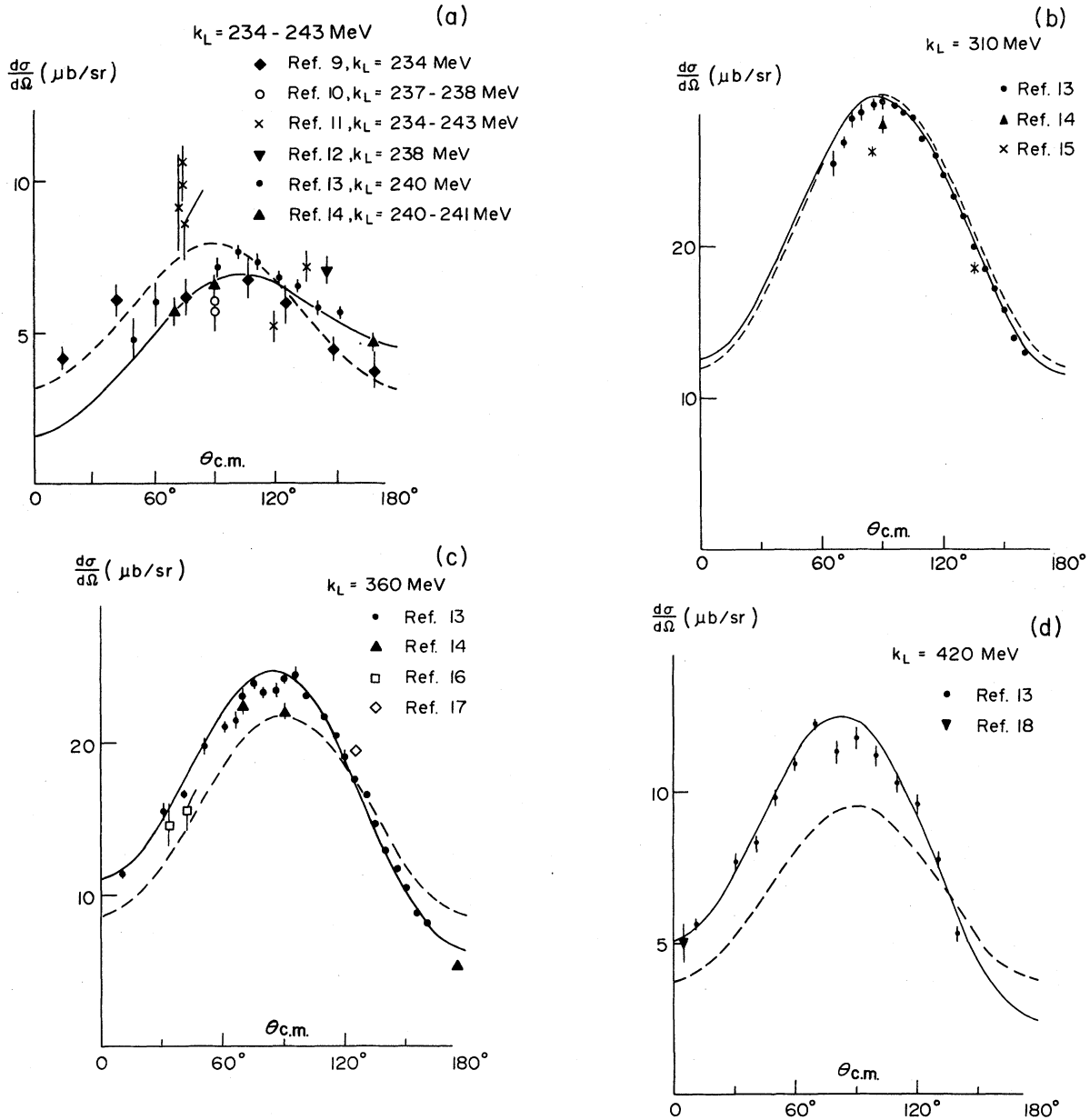


FIG. 3. Differential cross sections for $\gamma p \rightarrow \pi^0 p$ in the two-body c.m. frame. Solid curves correspond to the Berends-Donnachie multipole fit (Ref. 6); dashed curves correspond to keeping the $M_{1+}(\frac{3}{2})$ multipole alone. Statistical errors only indicated on graphs.

$$H_{\Delta h} = \gamma(E)H_{\Delta} + \delta W + W_{\pi} + V_{sp}, \quad (14)$$

$$\gamma(E) = \partial D(E) / \partial E, \quad (15)$$

$$H_{\Delta} = K_{\Delta} + V_{\Delta} + H_{A-1}. \quad (16)$$

Here, \vec{k} and \vec{q} are the photon and pion momenta, respectively, in the nuclear c.m. frame, and the 0 in the state vectors indicates that the nucleus is in the ground state. The vertex operators in Eq. (13) are

written in terms of the relative πN and γN momenta,

$$\vec{k}^* = \frac{E_k + k/A}{\sqrt{s_k}} \left[\vec{k} - \frac{k}{E_k + k/A} \vec{p}_i \right], \quad (17a)$$

$$\vec{q}^* = \frac{E_q + \omega_q/A}{\sqrt{s_q}} \left[\vec{q} - \frac{\omega_q}{E_q + \omega_q/A} \vec{p}_f \right], \quad (17b)$$

where \vec{p}_i and \vec{p}_f are the initial and final momenta of the target nucleon in the nuclear rest frame. The nucleon energies, E_k and E_q , and the invariant two body masses, s_k and s_q , are evaluated using frozen nucleus kinematics. The form of the many-body Δ -hole Hamiltonian has been described many times before,¹⁹ so we give here only a very brief summary. The Δ -Hamiltonian H_Δ incorporates Δ propagation effects through the kinetic energy operator K_Δ and the binding effects through the potential V_Δ and hole energy H_{A-1} . Pauli blocking of Δ decay in the medium is given by δW ; this reduces the free space decay width $\Gamma(E)/2$ contained in $D(E)$, Eq. (4), and shifts the resonance up in energy. The term W_π describes intermediate pion propagation in the presence of the nuclear ground state; this term corresponds to pion multiple scattering or, equivalently, to iteration of the optical potential in pion-nucleus scattering. All these terms taken together constitute the full first order optical potential, including binding, recoil, and exchange effects. They are evaluated microscopically in the space of Δ -hole configurations. In contrast, the last term in the Δ -hole Hamiltonian $H_{\Delta h}$, the spreading potential V_{sp} , is a phenomenological term which represents coupling to multihole intermediate channels. We take this to be a complex (optical) potential for the Δ proportional to the local density:

$$V_{sp}(r) = V_C \frac{\rho(r)}{\rho(0)} + V_{LS} \mu r^2 e^{-\mu r^2} 2\vec{L}_\Delta \cdot \vec{\Sigma}_\Delta. \quad (18)$$

The central and spin-orbit parameters V_C and V_{LS} , respectively, have been extracted²⁰ from analysis of pion elastic scattering on ${}^4\text{He}$, ${}^{12}\text{C}$, and ${}^{16}\text{O}$. The central part has a large imaginary part; both phenomenological analyses and microscopic calculations indicate that this is due to pion absorption through the $\Delta N \rightleftharpoons NN$ reaction. The parameters V_C and V_{LS} are nearly energy independent, and the values used in our calculations are given in Table I, together with the central strength of the binding potential V_Δ .

As described previously,¹ Eq. (13) is evaluated in a partial-wave doorway basis:

$$\sigma_{00}^L = \frac{1}{D(E) - H_{00}^L - \frac{H_{01}^L H_{10}^L}{D(E) - H_{11}^L - \frac{H_{12}^L H_{21}^L}{D(E) - H_{22}^L - \dots}}} \quad (28)$$

We have shown previously that this converges very rapidly for light nuclei.^{1,19} In this representation the new information accessible in principle in the

TABLE I. Δ -nucleus interaction parameters (taken from Ref. 20).

	V_Δ (MeV)	V_C (MeV)	V_{LS} (MeV)	μ (fm ⁻²)
${}^4\text{He}$	-75	40-35i	-4.6-1.8i	0.25
${}^{12}\text{C}$	-55	22.5-45i	-10-4i	0.35

$$\langle \vec{q}; 0 | T_\Delta | \vec{k}, \lambda; 0 \rangle = \sum_L \lambda Y_{L\lambda}^*(\hat{q}) T_\Delta^L, \quad \lambda = \pm 1 \quad (19)$$

$$T_\Delta^L \equiv (N_L^\dagger N_L)^{-1} \langle \tilde{D}_0^L | G_{\Delta h}(E) | D_\gamma^L \rangle, \quad (20)$$

$$G_{\Delta h}(E) = [D(E) - H_{\Delta h}]^{-1}. \quad (21)$$

Here, \hat{k} has been chosen as the polar axis, and the pion and photon doorway states are

$$|D_0^L\rangle \equiv N_L F_{\pi N \Delta} |(\vec{q})_L; 0\rangle, \quad (22)$$

$$|D_\gamma^L\rangle \equiv N_L^\dagger F_{\gamma N \Delta} |(\vec{k}, \lambda)_L; 0\rangle. \quad (23)$$

A complete set of biorthogonal, normalized states is built upon the pion doorway state by repeated application of $H_{\Delta h}$:

$$|D_n^L\rangle = N_n^L \left\{ H_{\Delta h} |D_{n-1}^L\rangle - \sum_{j=0}^{n-1} |D_j^L\rangle H_{j,n-1}^L \right\}, \quad (24)$$

$$H_{ij}^L \equiv \langle \tilde{D}_i^L | H_{\Delta h} | D_j^L \rangle. \quad (25)$$

This Lanczos construction puts the Hamiltonian matrix into tridiagonal form. Inserting the complete set to the right of $G_{\Delta h}$ in Eq. (20), we have

$$T_\Delta^L = (N_L^\dagger N_L)^{-1} \sum_n \sigma_{0n}^L \langle \tilde{D}_n^L | D_\gamma^L \rangle, \quad (26)$$

$$\sigma_{0n}^L \equiv \langle \tilde{D}_0^L | G_{\Delta h}(E) | D_n^L \rangle. \quad (27)$$

The diagonal term σ_{00}^L is equivalent to the (on-shell) pion-nucleus elastic scattering partial wave amplitude and yields the scattering phase shifts of the asymptotic pion wave function. It has the continued fraction representation

(γ, π^0) reaction is the off-diagonal terms σ_{0n}^L . These are equivalent to the pion scattering wave function and will distinguish between phase equivalent

models of π -nucleus scattering (same σ_{00}). Within the model, these are evaluated by a recursion relation

$$\begin{aligned}\sigma_{01}^L &= \frac{1}{H_{10}^L} \{ \sigma_{00}^L [D(E) - H_{00}^L] - 1 \}, \\ \sigma_{0,n+1}^L &= \sigma_{0,n}^L \frac{D(E) - H_{nn}^L}{H_{n+1,n}^L} \\ &\quad - \sigma_{0,n-1}^L \frac{H_{n-1,n}^L}{H_{n+1,n}^L}, \quad n \geq 1.\end{aligned}\quad (29)$$

The weights for the σ_{0n}^L in $T_{\gamma\pi}^L 0$ are the overlaps between the photon and pion doorways, $\langle \tilde{D}_n^L | D_\gamma^L \rangle$. We saw in Ref. 1 that $\langle \tilde{D}_0^L | D_\gamma^L \rangle$ is close to unity for peripheral and semiperipheral partial waves. Therefore, Eq. (26) implies that there is little sensitivity to the dynamics once the model is constrained by pion scattering. On the other hand, $\langle \tilde{D}_0^L | D_\gamma^L \rangle$ is small (e.g., ~ 0.3 for the 1^+ wave in ^{16}O with $T_\pi = 140$ MeV) for the central partial waves, so that the associated partial wave amplitudes may differ markedly, even for theories providing a rather simi-

lar description of pion elastic scattering. Of course, a partial wave analysis of coherent π^0 photoproduction would require far better data than presently exist. Thus, it is extremely important in comparing theoretical results for the (γ, π^0) process to critically compare the associated predictions for pion scattering.

The contribution of the various terms in $H_{\Delta h}$ to the doorway state matrix element H_{00}^L has been discussed previously in great detail. The reader is referred to Refs. 1 and 19 for further discussion. We repeat here only the important fact that, since V_{sp} has a strength comparable to the free space half-width (see Table I), the coupling to the absorption channel modifies the production amplitude strongly. Although V_{sp} is itself energy independent, its effect on the photoproduction amplitude has a strong energy dependence. For example, it increases damping of the pion wave function far from resonance and decreases it near the resonance. Also, the importance of this higher order effect implies that the DWIA approach is not quantitatively accurate. We can see this directly by rewriting Eq. (13) in terms of the pion scattering wave function

$$\langle \psi_{\vec{q}}^{(-)} | = \langle \vec{q}; 0 | \{ F_{\pi N \Delta}^\dagger G_{\Delta h}(E) F_{\pi N \Delta} P_0 G_\pi^0(E) + 1 \}, \quad (30)$$

$$G_\pi^0 = \frac{P_0}{E^+ - k_\pi - H_A}, \quad (31)$$

where G_π^0 is the free pion propagator with the nucleus in the ground state. Using the explicit form of the rescattering operator,

$$W_\pi = F_{\pi N \Delta} P_0 G_\pi^0 P_0 F_{\pi N \Delta}^\dagger, \quad (32)$$

we have

$$\langle \vec{q}; 0 | T_\Delta | \vec{k}, \lambda; 0 \rangle = \langle \psi_{\vec{q}}^{(-)}; 0 | F_{\pi N \Delta}^\dagger \frac{1}{D(E - H_\Delta) - \delta W - V_{sp}} F_{\gamma N \Delta} | \vec{k}, \lambda; 0 \rangle. \quad (33)$$

The operator inside the expectation value in Eq. (33) is the effective medium amplitude for π^0 photoproduction. V_{sp} , along with H_Δ and δW , is contained in this amplitude as well as in the distorted wave of the outgoing pion, Eq. (30). The Δ - h approach takes them into account in a consistent fashion. The standard impulse approximation operator including recoil in the vertices and the Δ propagator would be

$$(t_{\gamma\pi^0})_{\text{impulse}} = F_{\pi N \Delta}^\dagger \frac{1}{D(E - K_\Delta)} F_{\gamma N \Delta}. \quad (34)$$

The important spreading effect, in addition to binding and Pauli effects, is missing. We shall return to these points below in comparing with other calculations.

As noted in Sec. II, there are important background contributions to π^0 photoproduction, both in the resonant $M_{1+}(\frac{3}{2})$ multipole and in the background multipoles. Consequently, our nuclear amplitude becomes

$$T_{\gamma\pi^0} = T_B + T_{B\Delta} + e^{i\phi} T_\Delta, \quad (35)$$

where T_B represents background coherent π^0 photoproduction in the impulse approximation and the phase factor $e^{i\phi}$ modifies the (free space) $\gamma N \Delta$ vertex as in Sec. II. The second term $T_{B\Delta}$ corresponds to coherent π^0 photoproduction through the background term, with the π^0 rescattering through the Δ -hole channel. In other words, $(T_B + T_{B\Delta})$

represents DWIA for the background amplitude, our assumption being that the important medium effects are manifested only in the Δ -nucleus dynamics. These terms are illustrated in Fig. 4. Note that $T_{B\Delta}$ can be considered as a $\gamma\Delta h$ vertex correction in the medium. For the $M_{1+}(\frac{3}{2})$ background, we have, following Eq. (7),

$$(T_B^{M_{1+}} + T_{B\Delta}^{M_{1+}})_L = \mathcal{A}_B (N_L^Y N_L)^{-1} \langle \tilde{D}_0^L | G_{\Delta h} W_\pi + 1 | D_\gamma^L \rangle \quad (37)$$

$$= \mathcal{A}_B (N_L^Y N_L)^{-1} \sum_{m=0} \left\{ \delta_{m0} + \sum_n \sigma_{0n} (W_\pi)_{nm} \right\} \langle \tilde{D}_m^L | D_\gamma^L \rangle. \quad (38)$$

This is calculated easily using the previous results. The nonresonant multipole background terms are evaluated straightforwardly in a distorted wave impulse approximation.

IV. RESULTS AND COMPARISON WITH DATA

Various of the dynamical ingredients discussed above affect strongly even the overall magnitude of the (γ, π^0) cross section. First, the medium modifications of the resonant photopion production operator greatly reduce the cross section. This is demonstrated in Fig. 5, where we show the total $^{12}\text{C}(\gamma, \pi^0)^{12}\text{C}$ cross section, keeping only the resonant multipole. The DWIA result, defined by using Eq. (34) in Eq. (33), is substantially larger than the full calculation. Consequently, a consistent treatment of many-body effects in the production operator and in the pion optical potential (which is automatic in the Δ - h approach) is essential for an accurate calculation of coherent π^0 photoproduction. All remaining calculations shown in this paper

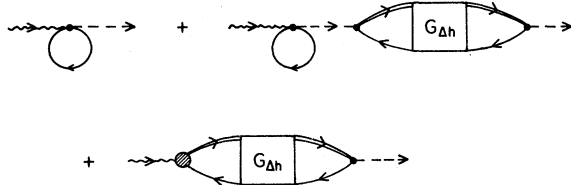


FIG. 4. Nuclear coherent photoproduction, including background and resonant production.

$$\langle \vec{q}; 0 | T_B^{M_{1+}} + T_{B\Delta}^{M_{1+}} | \vec{k}, \lambda; 0 \rangle = \mathcal{A}_B \langle \psi_{\vec{q}}^{(-)}; 0 | F_{\pi N \Delta}^\dagger F_{\gamma m \Delta} | \vec{k}, \lambda; 0 \rangle. \quad (36)$$

Using again the explicit form for W_π , the partial wave amplitude has the form

will be based upon the full amplitude defined by Eq. (13).

In Fig. 6, the total coherent π^0 photoproduction cross section on ^{12}C is shown keeping the full production operator, i.e., the resonant multipole $M_{1+}(\frac{3}{2})$ and all other multipoles, as discussed in Sec. II. Comparison is made with the Bonn data of Arends *et al.*²¹ However, it must be stressed that the data include not only coherent π^0 photoproduc-

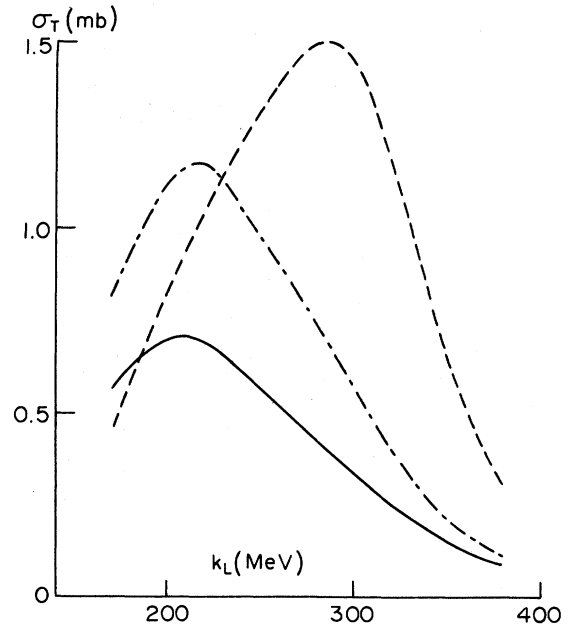


FIG. 5. Total cross section for coherent π^0 production from ^{12}C , keeping only the $M_{1+}(\frac{3}{2})$ multipole. Solid line is the Δ -hole result. Dashed curve represents the impulse approximation, while the dotted-dashed curve is the distorted wave impulse approximation result.

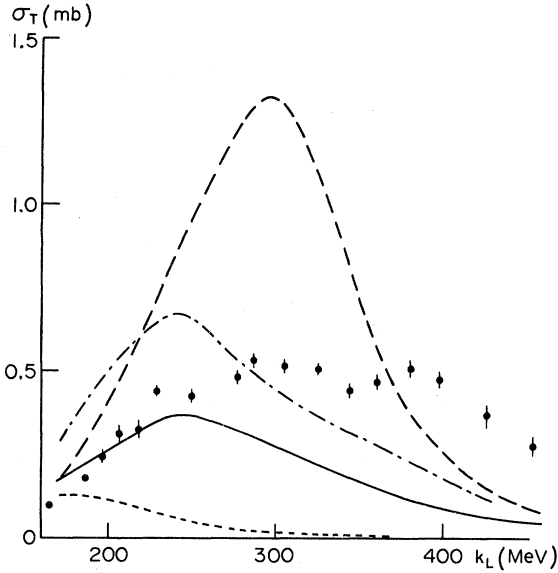


FIG. 6. Total cross section for coherent π^0 photoproduction from ^{12}C . Data from Ref. 21. Calculated results now include full photoproduction amplitude: solid line is the full result, dashed line is the impulse approximation, and dotted-dashed line is that with no Δ spreading potential. The short-dashed line is the result obtained in the absence of resonant production.

tion but also π^0 production accompanied by excitation of particle stable target states. The resulting overestimate of the coherent cross section is expected to be most severe at the higher photon energies, where larger momentum transfers to the nucleus are involved. Our calculation agrees reasonably well with the data for $k_L \leq 250$ MeV and falls significantly below for higher energy. The calculation with no spreading potential is also shown in the figure. Below 300 MeV, the $V_{sp}=0$ result is even larger than the upper bound provided by the Bonn data. Thus, a strong spreading potential is required. While our model is consistent with the data, obviously a clean separation of the coherent π^0 cross section is needed for a quantitative test. Finally, Fig. 6 also shows the contribution from nonresonant coherent π^0 photoproduction alone (i.e., $T_\Delta=0$); this represents an appreciable part of the cross section at the lower energies.

A troubling point is that the low energy $\gamma p \rightarrow \pi^0 p$

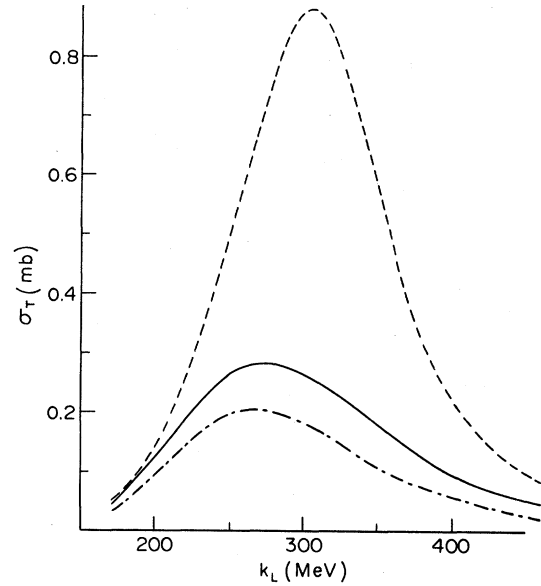


FIG. 7. Total cross section for coherent π^0 photoproduction from ^4He . Solid line is the full calculation; dashed is the impulse approximation. The dotted-dashed curve gives the result without recoil at the $\gamma N\Delta$ and $\pi N\Delta$ vertices.

data are not in very good shape. For a photon energy of about 240 MeV, the Berends-Donnachie multipole fit,⁶ which we use, fits the Bonn data¹³ but not the data of Govorkov *et al.*⁹ [see Fig. 3(a)]. The latter extend to smaller angles, which is the angular region in which the nuclear coherent $\gamma\pi^0$ cross section peaks (as we shall see shortly). Clearly, if the Govorkov *et al.*⁹ data are correct, our calculation of the nuclear coherent cross section will be much too small.

While there are no data yet on the total $^4\text{He}(\gamma, \pi^0)^4\text{He}$ cross section, we show our prediction in Fig. 7. Note that the cross section is almost as large as that for ^{12}C , because the nuclear form factor falls off more slowly with momentum transfer. We show in Fig. 7 the result obtained with the neglect of recoil at the $\gamma N\Delta$ and $\pi N\Delta$ vertices. The recoil effect is very large and must be included in any quantitative calculation. This is easily seen in impulse approximation. Using Eq. (17), we obtain

$$\langle 0 | \vec{S}^\dagger \cdot \vec{q} * \hat{\epsilon}_{\vec{k}\lambda} \cdot \vec{S} \times \vec{k} * e^{i\vec{Q} \cdot \vec{k}} | 0 \rangle = \frac{2}{3} C \hat{\epsilon}_{\vec{k}\lambda} \cdot \vec{k} \times \vec{q} \left\{ \left[1 + \frac{a+b}{2} \right] F(Q) - \frac{a+2b}{2} M(Q) \right\}, \quad (39)$$

where

$$a = (1 - 1/A) \frac{k}{E_k + k/A}, \quad (40)$$

$$b = (1 - 1/A) \frac{\omega_q}{E_q + \omega_q/A},$$

$$c = \frac{(E_k + k/A)(E_q + \omega_q/A)}{\sqrt{s_q s_k}}.$$

$F(Q)$ is the nuclear ground state form factor, $F(0) = A$, and $M = 0$ for closed shell nuclei such as ^4He and ^{16}O , while for ^{12}C

$$M_{^{12}\text{C}} = 2 \langle R_{11} | \frac{j_1(Qr)}{Qr} | R_{11} \rangle, \quad (41)$$

where R_{11} is the radial $1p$ -shell wave function. This is small compared to the $F(Q)$ term in the forward direction. In closed shell nuclei, our result, Eq. (39), is essentially the same as that obtained by Saharia and Woloshyn.⁴ The correction factor is also relatively independent of target mass, and the nuclear ground state form factor $F(Q)$ approximately factors out of the entire amplitude. These large recoil effects at the vertices (Fig. 7) must be distinguished from those in the Δ propagator. The latter shift the position of the peak through

$$\langle D_0^L | K_\Delta | D_0^L \rangle$$

in Eq. (28) and broaden it slightly through the fluctuation term

$$\langle D_0^L | K_\Delta | D_1^L \rangle \langle D_1^L | K_\Delta | D_0^L \rangle$$

in Eq. (28). The significant increase in the cross section comes only from the vertex recoil factors.

We now turn to a comparison with the existing differential cross section data. In Fig. 8, we show two sets of data for $^{12}\text{C}(\gamma, \pi^0)^{12}\text{C}$ for photon energies $k_{\text{lab}} \approx 240$ MeV. The old Davidson data²² have long been the subject of some controversy. Clearly, the two data sets are in considerable disagreement. Our calculation with the complete $\gamma N \rightarrow \pi^0 N$ amplitude is about a factor of 2 smaller than the Davidson data.²² The phenomenological doorway calculation of Saharia and Woloshyn⁴ is about 15% larger than our calculation, while that of Klingenberg and Huber³ is about a factor of 2 smaller. Note again that the full result is much smaller than either the impulse approximation result or the result with no spreading potential. In comparing with the Bonn data,²¹ we see that the calculated cross section lies about 20% above the data at the peak and below the data at large angles. However, two problems with the measurement must be kept in mind in drawing conclusions. First, as noted above, the data include

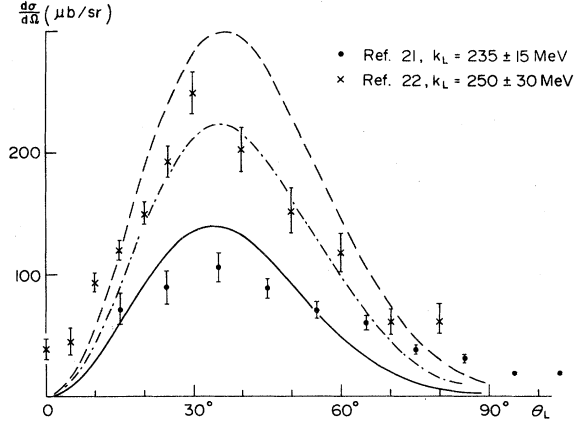


FIG. 8. Angular distribution for $^{12}\text{C}(\gamma, \pi^0)^{12}\text{C}$ for photon energy $k_L \approx 235$ MeV. Theoretical curves are the same as those in Fig. 6. The Davidson data have been corrected to take into account changes in the $\gamma p \rightarrow \pi^0 p$ cross section used for normalization of the nuclear cross section (E. Booth, J. Miller, and B. L. Roberts, private communication).

photoproduction accompanied by excitation of particle stable target states. This will increase the measured cross section, especially at large angles. Second, the π^0 angular resolution ranged from 35° (FWHM) for $T_{\pi^0} = 10$ MeV to 15° (FWHM) for $T_{\pi^0} = 300$ MeV. If our theoretical angular distribution is folded with the angular resolution appropriate for ~ 100 MeV pions, the peak value would be appreciably reduced, in rough agreement with the data. Furthermore, the folded cross section would increase for very small angles and for large angles. Given these uncertainties, there is no obvious disagreement between the Bonn data²¹ and the calculation including the full $\gamma N \rightarrow \pi^0 N$ amplitude and the spreading potential determined in pion scattering.

Recall from our discussion of the total cross section that this energy region is precisely that where the multipole fit does not well reproduce the Goukoff *et al.*⁹ forward angle $\gamma p \rightarrow \pi^0 p$ data. As can be seen from Fig. 3(a), the $M_{1+}(\frac{3}{2})$ multipole alone better fits the forward angle data at this energy. If we use only this multipole in the nuclear calculation (as in Fig. 5), our predicted angular distribution for $^{12}\text{C}(\gamma, \pi^0)^{12}\text{C}$ at 235 MeV is about a factor of 2 above that calculated with the full amplitude, bringing the result close to the Davidson data.²² Clearly, new experiments on the $\gamma N \rightarrow \pi^0 N$ process in this low energy region are needed for an accurate prediction of the nuclear cross section. Measurements at this energy of the coherent cross section on another nucleus, such as ^4He , would also be very helpful.

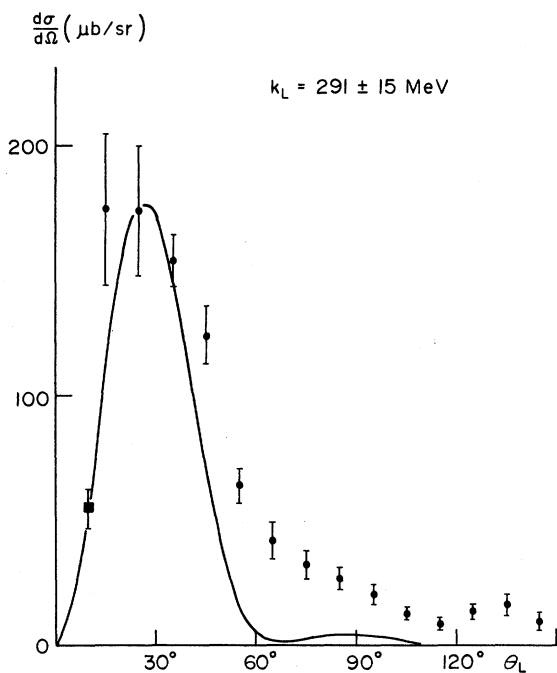


FIG. 9. Angular distribution for $^{12}\text{C}(\gamma, \pi^0)^{12}\text{C}$ for photon energy $k_L = 295$ MeV. Data are from Bonn (Ref. 21). The curve gives the result of the full calculation.

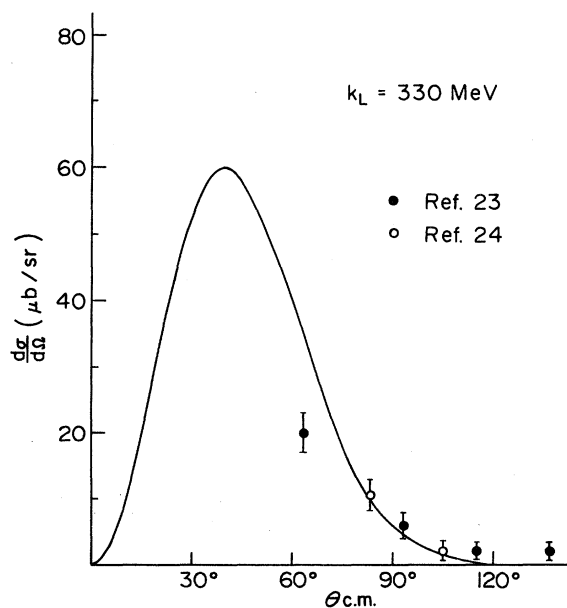


FIG. 10. Angular distribution for $^4\text{He}(\gamma, \pi^0)^4\text{He}$ for photon energy $k_L = 330$ MeV. The curve gives the result of the full calculation.

In Fig. 9, we show the full Δ -hole calculation for the $^{12}\text{C}(\gamma, \pi^0)^{12}\text{C}$ cross section near the resonance energy. The data are from Bonn.²¹ There is essentially no uncertainty in the elementary amplitude at these energies. Given the uncertainties in the coherent data discussed in the calculation above, the calculation agrees reasonably well with the data. Referring back to Fig. 6, we see that the spreading potential substantially reduces the cross section at this energy. Thus, the Δ -nucleus interaction parameters carried over from the pion scattering studies appear to be confirmed.

We see from Figs. 8 and 9 that the ^{12}C data are concentrated in the vicinity of the peak in the differential cross section. For ^4He , larger angle data (some of it obtained by measuring the recoiling ^4He nucleus) have been taken; these are more sensitive to details of the model. In Fig. 10, we show data and the full calculation for $^4\text{He}(\gamma, \pi^0)^4\text{He}$ in the resonance region ($k_\gamma = 330$ MeV). The data indicated by open circles are from Staples.²³ The rest are from LeFrancois *et al.*,²⁴ who detected the recoiling ^4He (we shall discuss this data set more fully below). The calculation agrees reasonably well with the large angle data, but is considerably larger than the datum at $\theta = 60^\circ$. Recall that the Δ -hole result appeared to do well at this energy in comparison with the Bonn data.²¹ A new measurement of this cross section spanning a larger angular range would provide a good test of the theory. Staples²³ also gives excitation functions for three large π^0 angles, where the cross section is very small. We compare them with our full calculation in Fig. 11. For $\theta_{\text{c.m.}} = 137^\circ$ and $k_L \geq 300$ MeV, the momentum transfer to the nucleus approaches that at which the ^4He charge form factor has a minimum. Since we use a harmonic oscillator description of ^4He , as do Saharia and Woloshyn⁴ and Oset and Weise,² we do not reproduce the nuclear form factor in this kinematical region. The comparison between theory and data looks fine at $\theta_{\text{c.m.}} = 115^\circ$ but is puzzling at $\theta_{\text{c.m.}} = 93^\circ$. Here the Staples data²³ indicate a pronounced rise above 300 MeV, although the nuclear form factor and elementary amplitude are smooth in this kinematical range. None of the calculations show such a peak (the curve shown in Ref. 2 was simply drawn incorrectly). Indeed, such a peak seems very unlikely, since it would necessarily correspond to strange behavior of the differential cross section near resonance. New measurements are called for. Also, it would be very nice to obtain photoproduction data on ^4He which cover the forward hemisphere, where the cross section is much larger (see Fig. 10).

Le Francois *et al.*²⁴ measured the $^4\text{He}(\gamma, \pi^0)^4\text{He}$ cross section for fixed ^4He recoil energy and

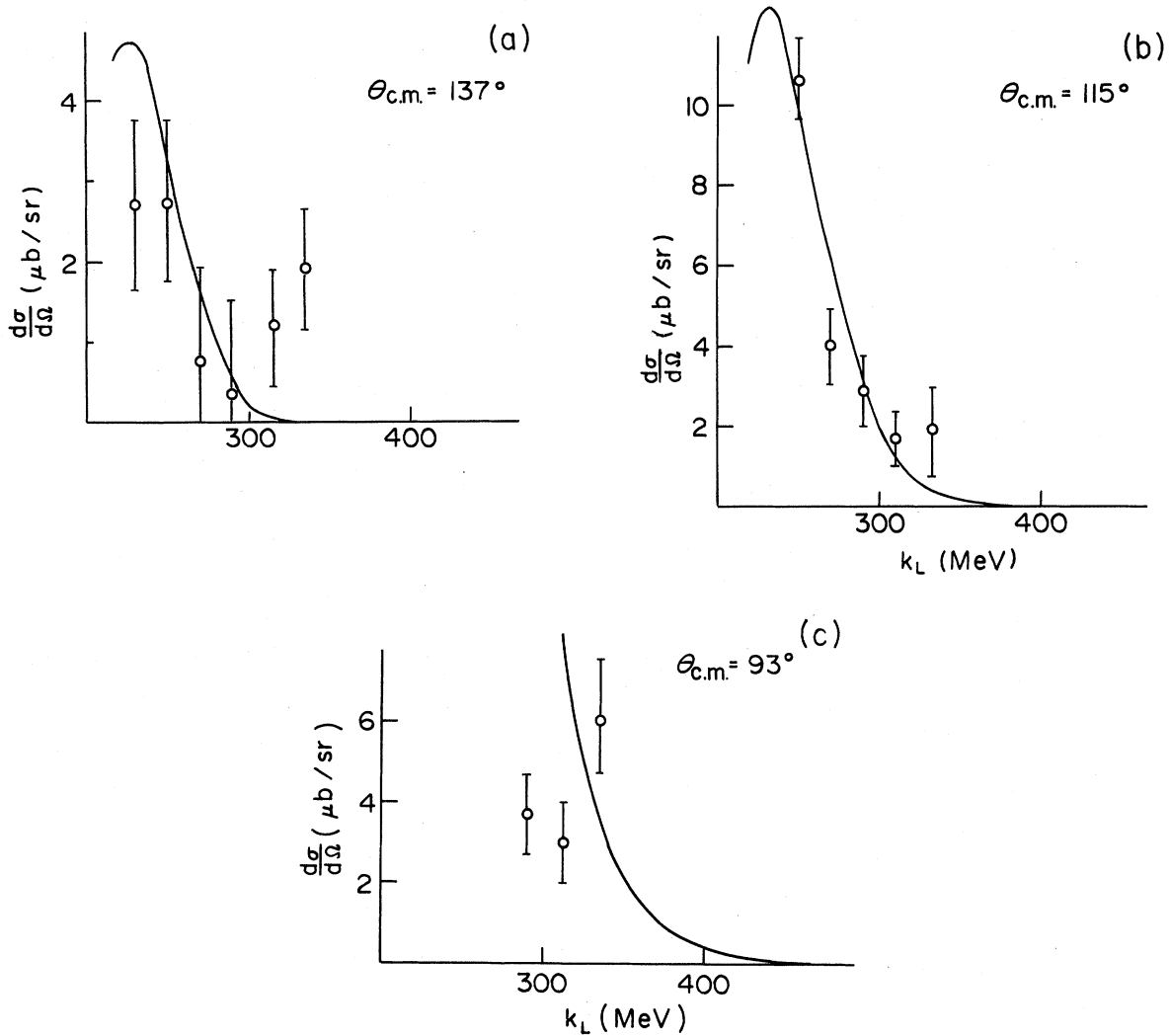


FIG. 11. Excitation function for ${}^4\text{He}(\gamma, \pi^0){}^4\text{He}$. Data from Ref. 23. Curves give the results of the full calculation.

momentum transfer Q as a function of incoming photon energy. These results for photon energies below 450 MeV are shown in Fig. 12. Note that the π^0 production angle is varying with energy in these data. For example, the 332 MeV point for $T_4 = 29$ MeV corresponds to a π^0 angle of $\theta_{\text{c.m.}} = 115.5^\circ$, a region where the differential cross section has dropped to only a few percent of its peak value (see Fig. 10). The errors shown are statistical only; according to the authors, a systematic error of $\sim \pm 14\%$ should be added. The Δ -hole calculations are shown both for the full elementary amplitude and for the $M_{1+}(\frac{3}{2})$ multipole only. For a given target recoil energy T_4 , the agreement between our full calculation and the data improves with increasing photon energy, which corresponds to smaller π^0 an-

gles. Again, inclusion of the background multipoles is seen to be important.

V. CONCLUSIONS AND SUMMARY

We are clearly not in a position to reach quantitative conclusions about Δ -nucleus dynamics by comparison with the existing coherent π^0 photoproduction data. First, more systematic data, spanning the resonance region and a range of target masses, are needed. Second, in the one case where a virtually identical measurement has been attempted at two different laboratories (see Fig. 8), the data disagree by about a factor of 2. Of course, the very poor energy resolution of the Davidson experiment²² may

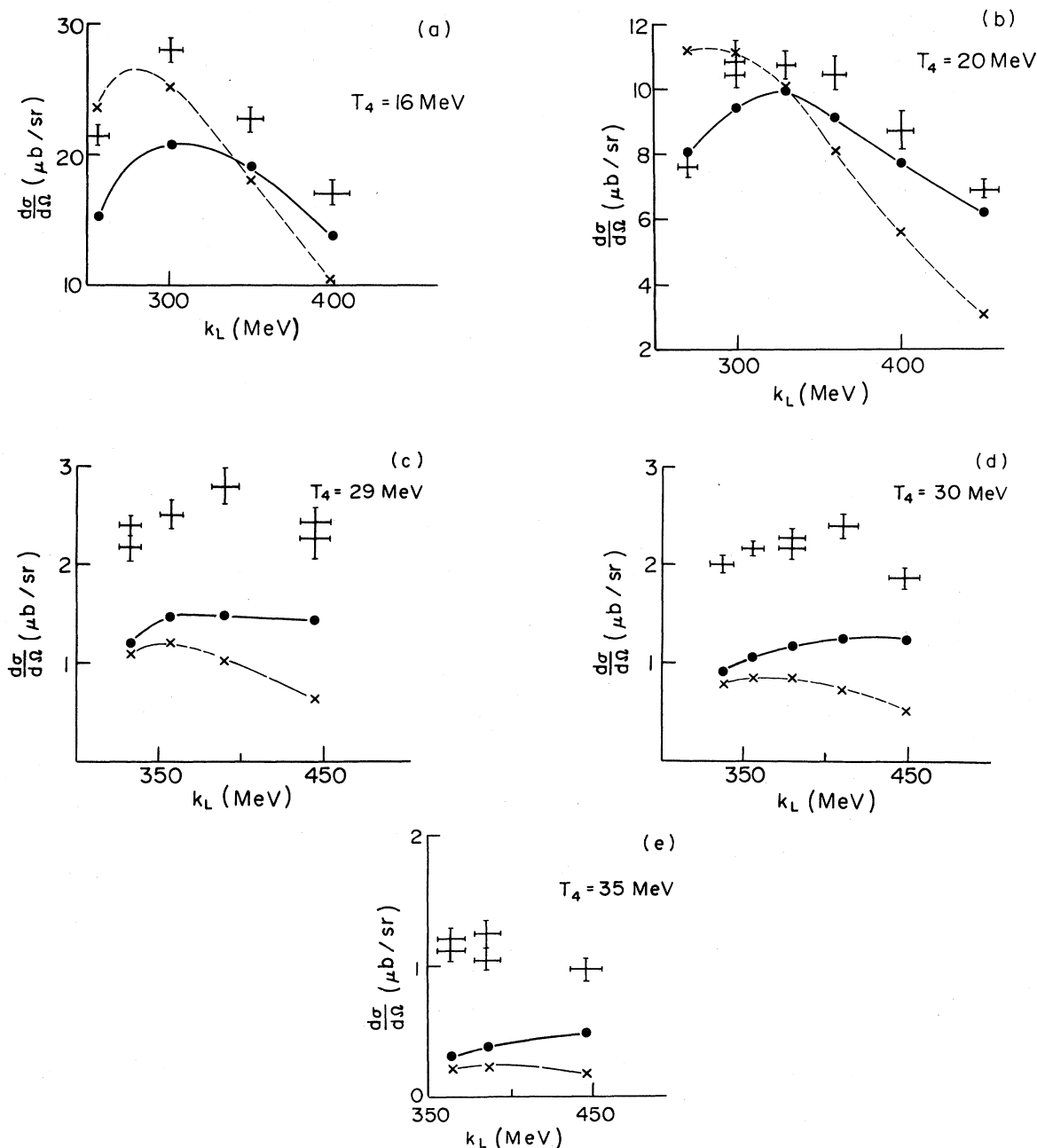


FIG. 12. Differential cross section for ${}^4\text{He}(\gamma, \pi^0){}^4\text{He}$ with fixed ${}^4\text{He}$ recoil energy, T_4 . Data from Ref. 24. Solid and dashed curves give the results of the calculation with the full photoproduction amplitude and with only the $M_{1+}(\frac{3}{2})$ multipole, respectively.

contribute to this; the nonvanishing forward cross section and the flattening of the large angle cross section may point to inclusion of some incoherent production. Finally, the uncertainty in the multipole fits to pion photoproduction on the nucleon, especially below the resonance and at forward angles, makes absolute calculation of the nuclear cross section difficult.

Using the full multipole fit, we do find reasonable agreement with the recent Bonn ${}^{12}\text{C}$ angular distribution.²¹ These data are consistent with a large reduction of the cross section caused by the Δ spreading potential, with the potential strength fixed by the pion scattering analyses. The large angle ${}^4\text{He}$ data were also reproduced reasonably well for energies close to the Δ peak. At the lower energies, we

again find considerable sensitivity to the dynamical model, but quantitative conclusions await clarification of the elementary $\gamma N \rightarrow \pi^0 N$ amplitude.

With regard to theoretical calculations of the process, we have identified several key ingredients. Dynamical effects such as the Δ spreading potential and Pauli blocking must be included. Oset and Weise² have done this in a manner similar to our approach, except that they attempt a microscopic evaluation of the spreading potential. A microscopic calculation leads to a nonlocal structure for the spreading potential, as one would expect. However, the important constraint on the Δ dynamics provided by the elastic pion scattering data should be observed. Saharia and Woloshyn⁴ incorporate these dynamical effects implicitly by directly taking over various parameters from fits to pion elastic scattering. This approach does not take into account the different structure of the Δ - h states excited by the photon and pion, which differ significantly in the central partial waves. Recoil at the γ/π absorption/production vertices enhances the cross section considerably (see Fig. 7). Saharia and Woloshyn⁴ have estimated this, and we agree with their conclusions. Recoil has not been treated in the same detail by Oset and Weise.²

Finally, we have seen that it is very important to include photoproduction from the nucleon in channels other than the Δ . This is certainly true away from the resonance, where the nonresonant multipoles interfere with the $M_{1+}(\frac{3}{2})$ to alter the differential cross section significantly. Oset and Weise² and Klingenberg and Huber³ have not included the background terms. The background is even significantly close to the resonance, particularly through the modification of the resonant $M_{1+}(\frac{3}{2})$ multipole (see Fig. 1). Our philosophy has been to separate the Δ and background production pieces, with the latter treated simply in distorted wave impulse approximation. In contrast to πN scattering, the $\gamma N \rightarrow \pi N$ experimental situation is rather unsettled. There exists no generally accepted multipole fit, which is necessary as input for a nuclear calculation. While there are much data for π^+ production, $\gamma p \rightarrow \pi^+ n$, the

low and intermediate energy $\gamma p \rightarrow \pi^0 p$ data are sparse and mainly restricted to the backward hemisphere, $\theta \gtrsim 60^\circ$. Clearly, calculations of photoproduction from a nucleus also require more information on photoproduction from neutrons as input.

The Δ production amplitude [see Eq. (33)] has all the medium modifications found important in pion scattering. The sum of these ingredients represents a "minimal" treatment of nuclear coherent π^0 photoproduction consistent with available information on Δ -nucleus interactions. Nevertheless, more detailed microscopic calculations may eventually prove essential. For example, medium corrections to the background production terms should be included. Also, local field modification of the effective $\gamma N \Delta$ vertex (Fig. 2), particularly by modification of the intermediate pion propagator, will alter the energy dependence of the photoproduction cross section (recall that this effective vertex already shifts the peak of $\text{Im}M_{1+}$ appreciably; see Fig. 1). However, it is known from studies²⁵ performed in the context of pion elastic scattering that these local field modifications are very difficult to calculate microscopically. We stress that such effects cannot be included by carrying over to the photoproduction process parameters fit in pion scattering.

In conclusion, we repeat that nuclear coherent π^0 photoproduction is rather sensitive to a variety of dynamical ingredients. However, the possibility that this process will improve our understanding of pion and/or Δ propagation awaits a significantly improved data base.

ACKNOWLEDGMENTS

We thank J. Arends and B. Mecking for sending us the Bonn data prior to publication, and for helpful discussions. We also acknowledge helpful discussions with N. Ohtsuka and H. Sagawa. This work was supported in part by the Foundation for Fundamental Research (FOM) and the Netherlands Organization for the Advancement of Pure Research (ZWO) and supported in part through funds provided by the U.S. Department of Energy (DOE) under Contract No. EY-76-C-02-3069.

¹J. H. Koch and E. J. Moniz, Phys. Rev. C **20**, 235 (1979).

²E. Oset and W. Weise, Nucl. Phys. **A368**, 375 (1981).

³K. Klingenberg and M. G. Huber, J. Phys. G **6**, 961 (1980).

⁴A. W. Saharia and R. M. Woloshyn, Phys. Rev. C **23**, 351 (1981).

⁵J. L. Goldberger and K. M. Watson, *Collision Theory*

(Wiley, New York, 1964), Chap. 9.

⁶F. A. Berends and A. Donnachie, Nucl. Phys. **B84**, 342 (1975).

⁷M. G. Olsson, Nucl. Phys. **B78**, 55 (1974).

⁸I. Blomqvist and J. M. Laget, Nucl. Phys. **A280**, 405 (1977).

⁹B. B. Govorkov, S. P. Denisov, and E. V. Minarik, J.

- Nucl. Phys. (USSR) 6, 370 (1968).
- ¹⁰D. B. Miller and E. H. Bellamy, Proc. Phys. Soc. (London) 81, 343 (1963).
- ¹¹G. Bernadini, A. O. Hanson, A. C. Odian, T. Yamagata, and L. B. Auerbach, Nuovo Cimento 18, 1203 (1960).
- ¹²P. Dougan, V. Ramsay, and W. Stiefler, Z. Phys. A 276, 155 (1976).
- ¹³H. Genzel, E. Hilger, G. Knop, H. Kemen, and R. Wedemeyer, Z. Phys. 268, 43 (1974).
- ¹⁴R. Morand, E. F. Erickson, J. P. Pahin, and M. G. Croissiaux, Phys. Rev. 180, 1299 (1969).
- ¹⁵E. R. Gray and A. O. Hanson, Phys. Rev. 160, 1212 (1967).
- ¹⁶W. S. McDonald, V. Z. Peterson, and D. R. Corson, Phys. Rev. 107, 577 (1957).
- ¹⁷P. Dougan, V. Ramsay, W. Stiefler, T. Kivikas, and K. Lugner, Z. Phys. A 274, 73 (1975).
- ¹⁸Y. Hemmi *et al.*, Phys. Lett. B43, 79 (1973).
- ¹⁹M. Hirata, J. H. Koch, F. Lenz, and E. J. Moniz, Ann. Phys. (N.Y.) 120, 205 (1979).
- ²⁰Y. Horikawa, M. Thies, and F. Lenz, Nucl. Phys. A345, 386 (1980).
- ²¹J. Arends *et al.*, Bonn report, 1982 (unpublished).
- ²²G. Davidson, MIT thesis, 1959 (unpublished).
- ²³J. W. Staples, Ph.D. thesis, University of Illinois, 1969 (unpublished).
- ²⁴J. Le Francois, P. Lehmann, and J. P. Repellin, Nuovo Cimento 65A, 333 (1970).
- ²⁵J. W. Van Orden, M. K. Banerjee, C. M. Schneider, and S. J. Wallace, Phys. Rev. C 23, 2157 (1981).